Transferable tight-binding parameters: An application to Ni and Ni-Al alloys

Marcel H. F. Sluiter and Prabhakar P. Singh
Chemistry and Materials Science Department, L-268, Lawrence Livermore National Laboratory, P.O. Box 808, Livermore, California 94550
(Received 23 November 1993)

The first-principles transformation of the linear muffin-tin orbitals (LMTO) into a tight-binding (TB) basis provides a reliable and very efficient method of obtaining the so-called Slater-Koster (SK) parameters, which can be used to gain insight into the electronic structure of complex systems, where conventional *ab initio* methods become too computer intensive. In this work we study the usefulness and the reliability of the SK parameters obtained from the TB-LMTO method, by examining their (i) transferability with changes in structural and chemical environments and (ii) applicability over a wide range of interatomic separations through explicit charge self-consistent LMTO calculations using Ni and Ni-Al systems as examples. We further test these parameters by comparing the densities of states and the effective pair interactions of Ni-Al system with the results of the more accurate Korringa-Kohn-Rostoker–coherent potential approximation method. We also compare our results with the SK parameters obtained empirically.

I. INTRODUCTION

Modeling of materials processes and properties is becoming more and more important in the field of materials science. Many properties of the perfectly crystalline ordered materials such as the lattice constants, elastic constants, heats of formation, etc., can be calculated accurately and reliably using *ab initio* electronic structure methods. However, many important physical properties are critically dependent on extended defects in crystalline or configurational order, such as, e.g., mechanical behavior, which is dictated largely by the generation and mobility of dislocations, and electrical conductivity, which is dependent on the state of short- or long-range order. These defects, which may exist only in low concentrations in an otherwise perfect crystal, pose a serious computational challenge because the conventional electronic structure methods become unwieldy when the number of atoms in the unit cell becomes large. It is here that elegant parametrizations of the electronic structure, such as the one provided by the tight-binding (TB) parameters, have great appeal. Such a parametrization reduces the computational effort by orders of magnitude, and can provide useful insight into the electronic structure of complex systems.

Traditionally, the TB parameters have been regarded as adjustable parameters which are determined by fitting to calculated energy eigenvalues at various points in the Brillouin zone. Such Slater-Koster (SK) parameters for elemental solids have been published by Papaconstantopoulos.[1] Another approach, followed in this paper, for obtaining the TB parameters uses the tight-binding formulation of the linear muffin-tin orbital Hamiltonian developed by Andersen *et al.*[2] The *ab initio* nature of the TB-LMTO approach makes empirical fitting unnecessary for obtaining the SK parameters.

The SK parameters must meet several conditions in order to describe the electronic structure of the distorted atomic configurations that occur in actual materials: (i) parameters must be valid for a wide range of atomic coordinations and environments, (ii) parameters must apply over a range of interatomic separations, and (iii) chemical effects between unlike atomic species must be accurately described. It is the purpose of this paper to demonstrate the usefulness and the reliability of the SK parameters obtained with the TB-LMTO method by examining their transferability with changes in structure and chemical environments, and their applicability over a wide range of interatomic separations. In the following we will regard the LMTO and the Korringa-Kohn-Rostoker coherent potential approximation (KKR-CPA) (Ref. 3) results as "exact."

The choice of Ni-Al alloys as examples was motivated by the availability of extensive first-principles electronic structure calculations for this alloy, and also by the fact that as an alloy of a transition metal and a normal metal it is not *a priori* obvious that a TB approach can provide an accurate electronic structure description.

The rest of the paper is organized as follows. In Sec. II we briefly describe the formalism for obtaining the SK parameters using the TB-LMTO method, and the effective pair interactions. Our results are described in Sec. III, followed by conclusions in Sec. IV.

II. FORMALISM

For obtaining the SK parameters using the TB-LMTO method, we start out with the Löwdin orthonormalized LMTO Hamiltonian,[2,3] $\mathbf{H}^{(2)}$ expressed in terms of the tight-binding first-order Hamiltonian $\mathbf{h}^{\beta}$,

$$\begin{aligned}\mathbf{H}^{(2)} &= \mathbf{E}_{\nu} + \mathbf{h}^{\beta}(1 + \mathbf{o}^{\beta}\mathbf{h}^{\beta})^{-1} \\ &= \mathbf{E}_{\nu} + \mathbf{h}^{\beta} - \mathbf{h}^{\beta}\mathbf{o}^{\beta}\mathbf{h}^{\beta} + \cdots ,\end{aligned} \tag{1}$$

where boldfaced symbols are matrices in site and angular momentum indices, β's are the screening parameters,

and the diagonal matrices $\mathbf{E}_\nu$ and $\mathbf{o}^\beta$ are the potential parameters determined self-consistently from the electronic structure calculations. In our calculations we keep terms that are correct only up to $(E-E_\nu)$, which results in the first-order Hamiltonian $\mathbf{H}^{(1)}$,

$$\mathbf{H}^{(1)} = \mathbf{E}_\nu + \mathbf{h}^\beta \,. \tag{2}$$

In terms of the potential parameters $\mathbf{C}$ and $\mathbf{\Delta}$, which are defined in Ref. 2, and the tight-binding structure constants $\mathbf{S}^\beta$, the Hamiltonian can be written as

$$\mathbf{H}^{(1)} = \mathbf{C} + \mathbf{\Delta}^{1/2}\mathbf{S}^\beta\mathbf{\Delta}^{1/2} \,. \tag{3}$$

The potential parameters, $\mathbf{C}$ and $\mathbf{\Delta}$, to be used in Eq. (3) are obtained from the self-consistent LMTO calculations.[2]

To take advantage of the Green's function formalism developed for empirical tight-binding approaches, we rewrite the electronic Hamiltonian, Eq. (3), as

$$H = \sum_{i,\lambda} |i\lambda\rangle \epsilon_i^\lambda \langle i\lambda| + \sum_{i,j,\lambda,\mu} |i,\lambda\rangle \beta_{ij}^{\lambda\mu} \langle j,\mu|, \tag{4}$$

where $|i\lambda\rangle$ denotes a state vector associated with site i and orbital λ, ϵ is the site and orbital diagonal on-site energy, and β represents the two-center hopping integral. The on-site energies ϵ_i and hopping integrals $\beta_{i,j}$ depend on the occupancy of the sites i and j. In many tight-binding studies only the diagonal disorder, associated with ϵ_i assuming the values ϵ^A or ϵ^B, is treated properly. Here, the off-diagonal disorder (ODD), associated with the disorder in the hopping parameters, is treated exactly within the single-site CPA framework according to the method by Blackman, Esterling, and Berk (BEB)[4] as formulated by Gonis and Garland.[5] In the BEB treatment matrix locators $\underline{g}_i$, Green's functions $\underline{G}_{ij}$, and hopping integrals are defined as

$$\underline{g}_i = \begin{pmatrix} x_i g^A & 0 \\ 0 & y_i g^B \end{pmatrix}, \tag{5}$$

$$\underline{G}_{ij} = \begin{pmatrix} x_i G_{ij} x_j & x_i G_{ij} y_j \\ y_i G_{ij} x_j & y_i G_{ij} y_j \end{pmatrix} \tag{6}$$

$$= \begin{pmatrix} G_{ij}^{AA} & G_{ij}^{AB} \\ G_{ij}^{BA} & G_{ij}^{BB} \end{pmatrix}, \tag{7}$$

$$\underline{\beta}_{ij} = \begin{pmatrix} \beta_{ij}^{AA} & \beta_{ij}^{AB} \\ \beta_{ij}^{BA} & \beta_{ij}^{BB} \end{pmatrix}, \tag{8}$$

where the locator $g^A = (z-\epsilon^A)^{-1}$, the Green's function $G = (z-H)^{-1}$, and the projection operator $x_i = 1 - y_i$ equals unity (zero) when site i is occupied by an $A(B)$ atom. The line under a function indicates that it is a matrix in terms of the site occupation. Note that the locators $\underline{g}_A$ and $\underline{g}_B$ cannot be inverted.

We now define an effective medium with its associated self-energy $\underline{\sigma}$ and coherent locator

$$\underline{g}^{\mathrm{CPA}} = (\underline{z} - \underline{\sigma})^{-1} \tag{9}$$

$$= \left[\begin{pmatrix} \underline{z} & 0 \\ 0 & \underline{z} \end{pmatrix} - \begin{pmatrix} \sigma_{ij}^{AA} & \sigma_{ij}^{AB} \\ \sigma_{ij}^{BA} & \sigma_{ij}^{BB} \end{pmatrix} \right]^{-1}, \tag{10}$$

such that the single-site-occupation averaged on-site Green's function $\langle \underline{G}_{00} \rangle$ is equal to the on-site Green's function of the effective medium $\underline{G}_{00}^{\mathrm{CPA}}$,

$$\langle \underline{G}_{00} \rangle = \underline{G}_{00}^{\mathrm{CPA}}. \tag{11}$$

It must be noted that $\sigma^{AB} = \sigma^{BA}$. The CPA on-site Green's function is most easily obtained in reciprocal space,

$$\underline{G}_{00}^{\mathrm{CPA}} = N_{\mathbf{k}}^{-1} \sum_{\mathbf{k}} (\underline{z} - \underline{\sigma} - \underline{\beta}_{\mathbf{k}})^{-1}, \tag{12}$$

where $\mathbf{k}$ is a reciprocal space vector in the first Brillouin zone and $N_{\mathbf{k}}$ is the number of reciprocal vectors in the first Brillouin zone. The hopping integrals can be Fourier transformed with

$$\underline{\beta}_{\mathbf{k}} = N^{-1} \sum_{i,j} \underline{\beta}_{ij} e^{i\mathbf{k}\cdot\mathbf{R}_{ij}}, \tag{13}$$

where $\mathbf{R}_{ij}$ is the vector connecting sites i and j, and where N is the number of sites.

The single-site-averaged on-site Green's function can be computed with[5]

$$\langle \underline{G}_{00} \rangle = \langle \{ \underline{1} - \underline{g}_i [(\underline{g}^{\mathrm{CPA}})^{-1} - (\underline{G}_{00}^{\mathrm{CPA}})^{-1}] \}^{-1} \underline{g}_i \rangle, \tag{14}$$

which simplifies to

$$\langle \underline{G}_{00} \rangle = \begin{pmatrix} \frac{1-c}{\sigma^{AA} - \epsilon_A - (G^{\mathrm{CPA},AA})^{-1}} & 0 \\ 0 & \frac{c}{\sigma^{BB} - \epsilon_B - (G^{\mathrm{CPA},BB})^{-1}} \end{pmatrix}, \tag{15}$$

where c denotes the concentration of the B species. The equality of Eqs. (12) and (15) implies that $G^{\mathrm{CPA},AB}$ and $G^{\mathrm{CPA},BA}$ vanish, which reflects the fact that a site cannot be occupied by both an A and a B atom simultaneously. Equation (11) is solved for the coherent locator with a modified iteration with average t-matrix approximation (IATA) scheme,[6,7] where the correction to the coherent locator $\Delta\underline{g}^{\mathrm{CPA}}$ is computed from

$$\Delta\underline{g}^{\mathrm{CPA}} = -\frac{\underline{g}^{\mathrm{CPA}} \langle \underline{t} \rangle \underline{g}^{\mathrm{CPA}}}{\underline{1} + \langle \underline{t} \rangle (\underline{G}^{\mathrm{CPA}} + \underline{g}^{\mathrm{CPA}})}, \tag{16}$$

where the site-averaged t matrix $\langle \underline{t} \rangle$ is given by

$$\langle \underline{t} \rangle = (1-c)\underline{t}_A + c\underline{t}_B \tag{17}$$

$$= (1-c)\{ \underline{G}_{ii}^{\mathrm{CPA}} + [\underline{1} - \underline{g}_A (\underline{g}^{\mathrm{CPA}})^{-1}]^{-1} \underline{g}_A \}^{-1} + c\{ \underline{G}_{ii}^{\mathrm{CPA}} + [\underline{1} - (\underline{g}_B^{\mathrm{CPA}})^{-1}]^{-1} \underline{g}_B \}^{-1}. \tag{18}$$

The iterations are carried out over the coherent locator rather than over the coherent potential because the latter becomes singular at concentration approaching zero or 1. For the first iteration we guess the coherent locator

according to $\underline{g}^{\mathrm{CPA}} = (1-c)\underline{g}_A + c\underline{g}_B$.

The generalized perturbation method (GPM) can be applied to the CPA with ODD by using the site-occupation matrix formulation of the appropriate Green's functions and t matrices. The effective pair interactions are given by

$$V_{ij}^{\lambda\mu} = -\frac{1}{2\pi}\mathrm{Tr}\sum_{\lambda,\mu}(\underline{X}_{ij,\lambda\mu}^{A} - \underline{X}_{ij,\lambda\mu}^{B})(\underline{X}_{ji,\mu\lambda}^{A} - \underline{X}_{ji,\mu\lambda}^{B}), \tag{19}$$

where $\underline{X}_{ij}^{A} = \underline{G}_{ij}^{\mathrm{CPA}}\underline{t}_A$, and where the trace Tr refers to a sum over the site-occupation matrix elements. λ and μ refer to the angular momentum indices. The effective pair interactions can be decomposed with regard to angular momentum according to

$$V_{ij}^{\lambda\mu} = -\frac{1}{2\pi}\mathrm{Tr}(\underline{X}_{ij,\lambda\mu}^{A} - \underline{X}_{ij,\lambda\mu}^{B})(\underline{X}_{ji,\mu\lambda}^{A} - \underline{X}_{ji,\mu\lambda}^{B}). \tag{20}$$

III. RESULTS AND DISCUSSION

In this section we describe the results of our study of the SK parameters in terms of (i) scaling with interatomic separations, (ii) on-site energies, (iii) transferability with change in structural environment, and (iv) transferability with change in chemical environment.

A. Scaling with interatomic separations

It is well known that the SK parameters depend on interatomic distance.[7] The most common relationship employed to take this distance scaling into account is the one derived by Andersen *et al.*[8] from the LMTO formalism:

$$\beta_{ll'M} = \beta_{ll'M}(d_0)\left[\frac{d}{d_0}\right]^{l+l'+1}, \tag{21}$$

where β represents a hopping parameter and d represents distance between the two nuclei. The validity of this ex-

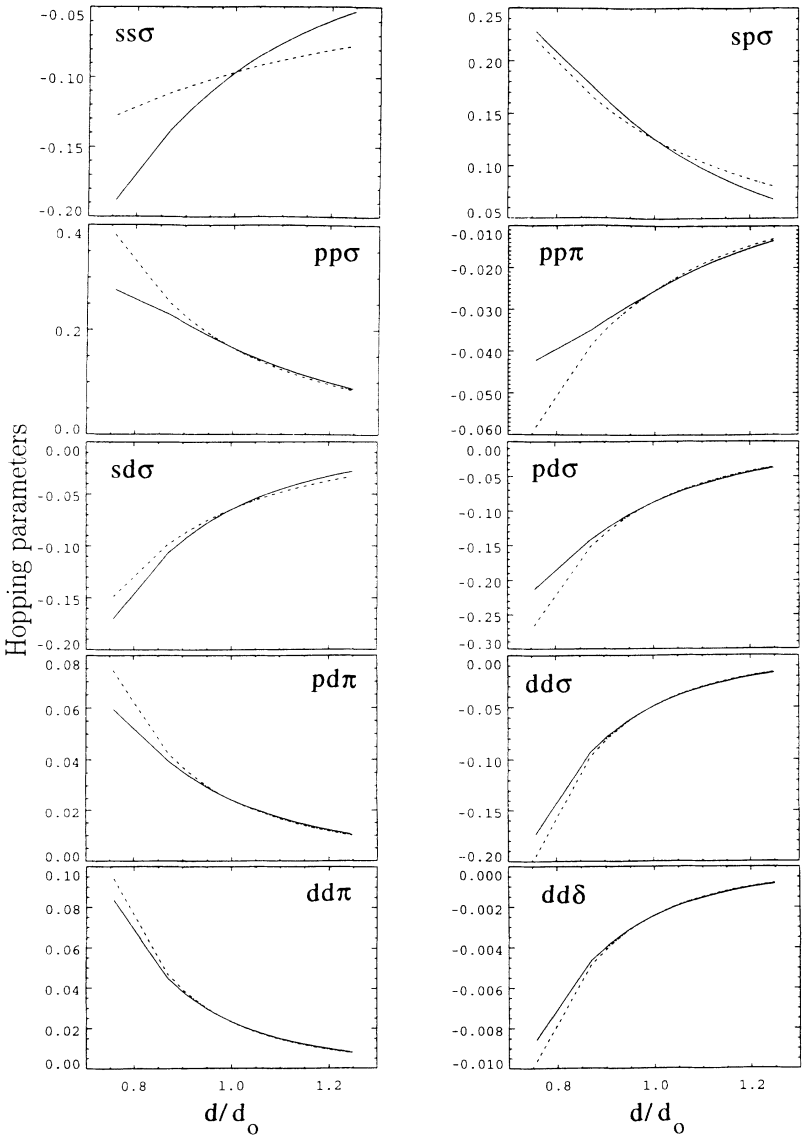

FIG. 1. Hopping parameters in the nearest-neighbor shell in fcc Ni as a function of interatomic distance as computed with Eq. (3) (dashed line) and as computed directly from the LMTO potential parameters (solid line).

pression was evaluated by performing LMTO calculations on fcc Ni at various lattice parameters and using the potential parameters to obtain SK parameters. These directly calculated SK parameters were compared with those extrapolated from the equilibrium lattice parameters using Eq. (21); the results are displayed in Fig. 1. As expected, Eq. (21) is especially accurate in the atomic limit (large d/d_0) and for large angular momentum $l+l'$. In previous work[9] it was concluded that Eq. (21) is valid for up to about 5% interatomic distance changes. Here, we find that the expression holds for essentially arbitrarily large expansions but breaks down at more than about 10% compression.

TABLE I. LMTO potential parameters (in Ry) of Ni with the fcc, bcc, and $A15$ crystalline structures.

	l	E_ν	C	Δ	γ
fcc	0	-0.4711	-0.3180	0.1862	0.4265
	1	-0.3118	0.7343	0.1739	0.1135
	2	-0.2104	-0.1821	0.0119	-0.0025
bcc	0	-0.4707	-0.3185	0.1858	0.4265
	1	-0.3133	0.7323	0.1736	0.1135
	2	-0.2096	-0.1815	0.0119	-0.0026
$A15$	0	-0.4806	-0.3207	0.1863	0.4267
	1	-0.3207	0.7325	0.1741	0.1135
	2	-0.2164	-0.1887	0.0119	-0.0025

B. On-site energies

Usually, the change of the on-site energies with the Wigner-Seitz (WS) radius is ignored. Here, it is found that the on-site energies can shift significantly with respect to each other (see Fig. 2). Therefore, when the WS radius changes, not only the hopping parameters but also the on-site energies must be adjusted. This can be conveniently accomplished within the TB-LMTO method by means of the potential parameter derivatives listed in Table VII of Ref. 2.

C. Transferability with change in structural environment

To examine the transferability of the SK parameters obtained with the TB-LMTO method we calculated the electronic structure of Ni in fcc, bcc, and $A15$ crystal structures at a Wigner-Seitz radius of 2.60 a.u. using the LMTO method. These three structures were selected because they reflect a wide variety of atomic environments. The fcc and the bcc are simple structures with 12- and 14-fold atomic coordinations, while $A15$ is one of the simplest complex structures with 12-fold coordination on some sites and 14-fold coordination on other sites. The potential parameters of relevance to the TB parametrization are given in Table I. It is clear that the variation in atomic environment has little influence on the potential parameters. As a consequence, when the potential parameters of bcc and $A15$ structures are used to compute the SK parameters of, say, fcc Ni only small variations are found, typically less than about 4 mRy in the on-site energies and less than 0.5 mRy in the hopping parameters (see Table II). This means that SK parameters for complicated structures with large unit cells can be computed with potential parameters from LMTO calculations on much simpler structures.

There are some noticeable differences between the TB-LMTO and the fitted SK parameters. The s and p on-site energies are much farther above the d on-site energies in the fitted SK parameters. Moreover, some hopping parameters have significantly different values or even different signs ($pp\pi$ in first shell, $dd\pi$ and $pd\pi$ in second shell). It appears that the higher s and p on-site energies in the fit are compensated for by larger hopping parameters. To some extent the larger hopping parameters in the fit result from the smaller WS radius (2.56 a.u.).

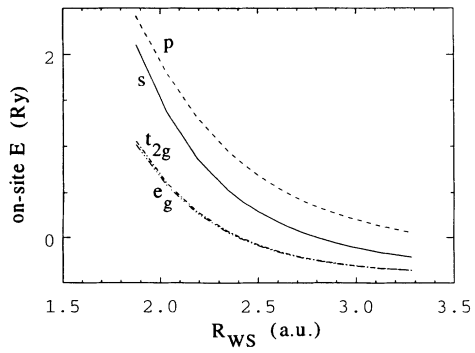

FIG. 2. On-site energies in fcc Ni as a function of WS radius as computed from the LMTO potential parameters

D. Transferability with change in chemical environment

It is by no means obvious that TB parameters obtained from pure elements would still be applicable within a concentrated alloy. As a check the LMTO potential parameters of both Ni and Al were computed for the pure fcc elements and for the $B2$ NiAl intermetallic compound; the results are listed in Table III. Clearly, at the same WS radii the potential parameters from the pure element and from the $B2$ NiAl calculation differ significantly. The differences are much reduced when the $B2$ NiAl potential parameters are evaluated in the vicinity of its own equilibrium WS radius. Nevertheless, it is clear that the potential parameters are much more sensitive to the chemical environment than to the crystalline structure.

1. Densities of states

Another verification of the applicability of the various TB parameters has been performed by calculating the densities of states (DOS's) of the fcc equiatomic alloys with the CPA. The TB results are compared with

TABLE II. Slater-Koster parameters in fcc paramagnetic Ni obtained from $A15$ (1), bcc (2), and fcc (3) LMTO potential parameters, and (4) as obtained from the fit to augmented-plane-wave results by Papaconstantopoulos (Ref. 1). To facilitate the comparison the fitted on-site energies have been shifted rigidly so as to match the TB-LMTO fcc t_{2g} on-site energy.

fcc	SK	(1)	(2)	(3)	(4)
[000]	s	0.163082	0.168288	0.169437	0.44342
	p	0.538837	0.544057	0.546883	0.89403
	t_{2g}	-0.157983	-0.150625	-0.151158	-0.15116
	e_g	-0.166814	-0.159480	-0.160033	-0.15431
$a/2$ [110]	$ss\sigma$	-0.078474	-0.078795	-0.078905	-0.09525
	$pp\sigma$	0.139982	0.140426	0.140846	0.21708
	$pp\pi$	-0.017498	-0.017553	-0.017606	0.01660
	$dd\sigma$	-0.041885	-0.041997	-0.042092	-0.03712
	$dd\pi$	0.017915	0.017963	0.018003	0.02629
	$dd\delta$	-0.001640	-0.001644	-0.001648	-0.00600
	$sp\sigma$	0.104397	0.104776	0.105005	0.14003
	$sd\sigma$	-0.055178	-0.055364	-0.055465	-0.03880
	$pd\sigma$	-0.074883	-0.075102	-0.075299	-0.04400
	$pd\pi$	0.017829	0.017881	0.017928	0.02377
a [100]	$ss\sigma$	-0.003243	-0.003256	-0.003261	-0.00065
	$pp\sigma$	0.006299	0.006319	0.006338	0.06220
	$pp\pi$	0.000000	0.000000	0.000000	0.00682
	$dd\sigma$	-0.002902	-0.002909	-0.002916	-0.00651
	$dd\pi$	-0.000252	-0.000253	-0.000254	0.00344
	$dd\delta$	0.000000	0.000000	0.000000	-0.00027
	$sp\sigma$	0.004261	0.004277	0.004286	0.01441
	$sd\sigma$	-0.002714	-0.002723	-0.002728	-0.01015
	$pd\sigma$	-0.004160	-0.004172	-0.004183	-0.01012
	$pd\pi$	-0.000297	-0.000298	-0.000299	0.00510

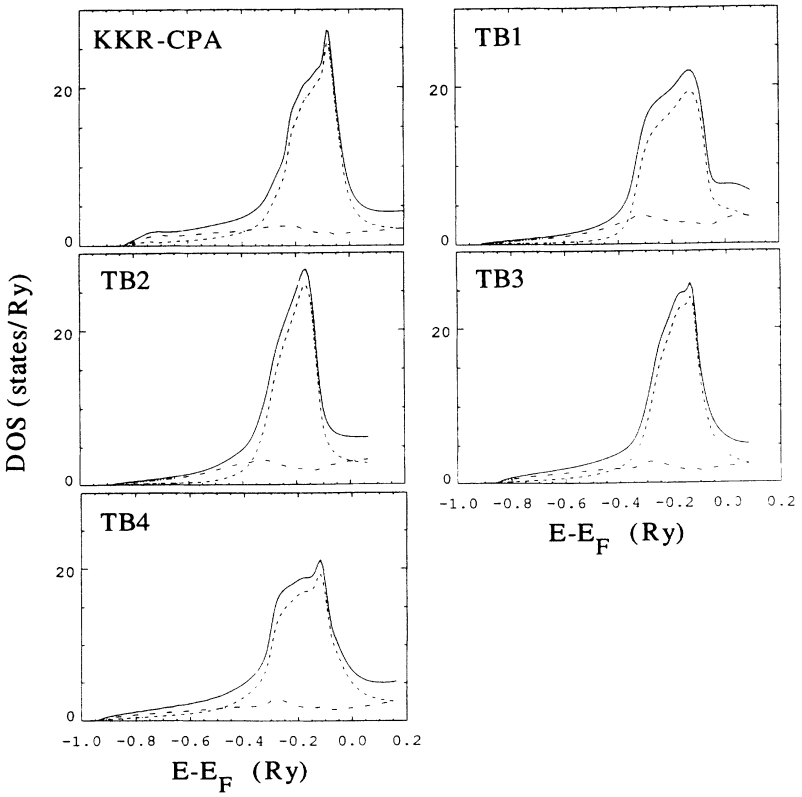

FIG. 3. DOS of fcc $Ni_{0.5}Al_{0.5}$ as obtained with the KKR-CPA and various TB approximations (see text). Total DOS (solid line), Ni partial DOS (dash-dotted line), and Al partial DOS (dash-triple-dotted line).

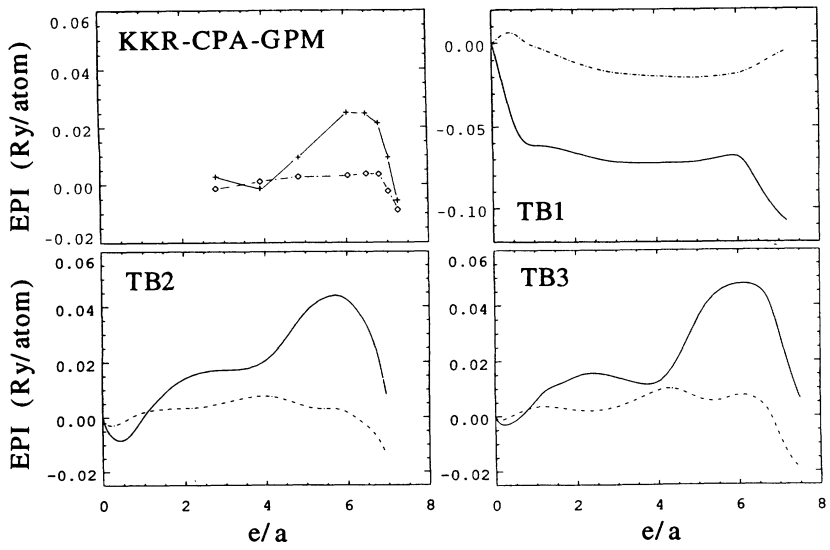

FIG. 4. First- (solid line) and second-nearest-neighbor EPI (dashed line) in bcc $Ni_{0.5}Al_{0.5}$ as a function of the electron/atom ratio as computed with the KKR-CPA with the frozen potential approximation, and as computed with various TB parametrizations. TB1: SK parameters from Ref. 1, TB2: TB-LMTO with potential parameters from fcc Ni and fcc Al, TB3: TB-LMTO with potential parameters from $B2$ NiAl.

a KKR-CPA result in Fig. 3. The DOS marked TB1 has been computed using the parameters for fcc Al and fcc paramagnetic Ni listed in Ref. 1 without any modifications. In comparison with the KKR-CPA results, the bandwidth is much larger and the Ni d band appears too low. These shortcomings can be somewhat mitigated by scaling the hopping parameters according to Eq. (21) for changes in the WS radius, and by rigidly shifting the Ni on-site energies down by 100 mRy with respect to the Al on-site energies. The results thus obtained are marked TB2.

It must be noted that a rigid shift of the on-site energies of one element generally is required because the data in Ref. 1 are given with reference to the muffin-tin zero which is different for each element, structure, and WS radius. The TB2 result has a slightly too narrow Ni d band which is still somewhat too far below the Fermi level and, related to this, there are too few states in the bottom of the band.

In TB3 the TB-LMTO was used with SK parameters from the pure elements rescaled with Eq. (21) for the change in the WS radius. The Ni d band is too narrow and too far below the Fermi level. It appears that the characteristic feature of the sharp peak at the upper edge of the Ni d band is correctly described. The SK parameters derived from the $B2$ NiAl structure give rise to the DOS marked TB4. Here, the d band is again too wide but otherwise the agreement with the KKR-CPA is

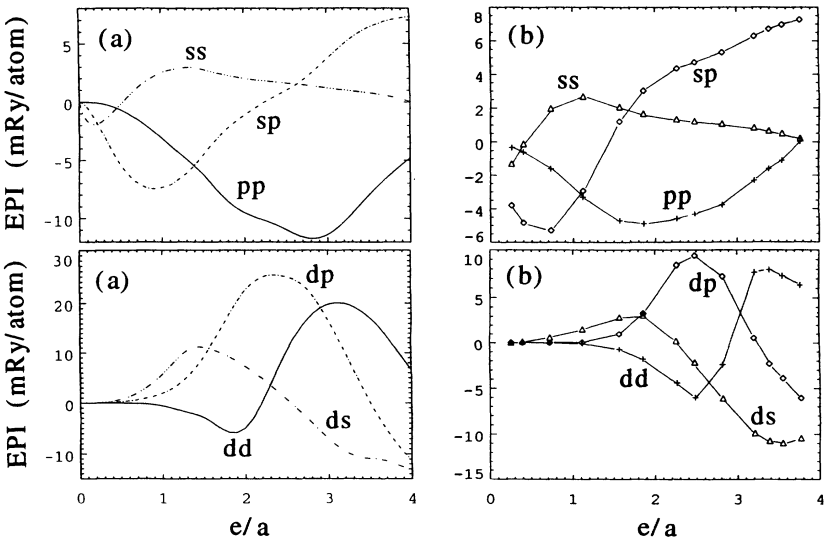

FIG. 5. Angular-momentum-decomposed nearest-neighbor EPI in fcc $Ni_{0.1}Al_{0.9}$ as a function of electron per atom ratio, as computed with (a) the SK parameters obtained from the TB-LMTO method (using the potential parameters from pure fcc elements) and (b) the KKR-CPA-GPM.

TABLE III. LMTO potential parameters (in Ry) of Ni as obtained from LMTO calculations on the fcc pure element and the B2 NiAl intermetallic compound. fcc: R_{WS}=2.60 a.u., $B2$ (1): R_{WS}=2.60 a.u., $B2$ (2): R_{WS}=2.683 a.u.

	l	E_ν	C	Δ	γ
fcc	0	-0.4711	-0.3180	0.1862	0.4265
	1	-0.3118	0.7343	0.1739	0.1135
	2	-0.2104	-0.1821	0.0119	-0.0025
(1)	0	-0.4151	-0.2825	0.1899	0.4266
$B2$	1	-0.2448	0.7707	0.1761	0.1134
	2	-0.1117	-0.0745	0.0131	-0.0036
(2)	0	-0.4405	-0.3256	0.1736	0.4250
$B2$	1	-0.2853	0.6632	0.1625	0.1128
	2	-0.1516	-0.1187	0.0113	-0.0037

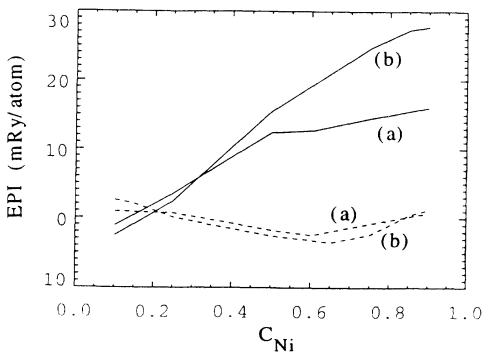

FIG. 6. First- (solid line) and second-nearest-neighbor EPI (dashed line) in fcc Ni-Al alloys as a function of composition as computed with (a) the KKR-CPA-GPM and (b) the SK parameters obtained from the TB-LMTO method (using the potential parameters from pure fcc elements).

fairly good. It is rather difficult to evaluate which TB DOS best approximates the KKR-CPA result and hence examining the DOS may not be very discriminating.

2. *Effective pair interactions*

A more critical test is provided by computing the effective pair interactions (EPI's) as defined in Eq. (19) by the generalized perturbation method.[10] The EPI's indicate the presence and nature of ordering or clustering in an alloy. Before we examine the transferability of the various SK parameters using Ni-Al, we would like to remind readers that the equiatomic Ni-Al alloys form an extremely stable bcc-based ordered intermetallic compound with the $B2$ (CsCl-type) structure. The occurrence of this phase implies that the nearest-neighbor EPI is strongly positive, as has indeed been found in KKR-CPA-GPM calculations.[11]

The question whether the various TB approaches correctly describe the nature of the chemical interactions (EPI's) in this alloy has been addressed in Fig. 4. It is clear that the SK parameters from Ref. 1 do not at all describe the EPI's in the actual Ni-Al system, as the computed values have the opposite sign. Moreover, the parameters cannot be adjusted by shifting the on-site energies of one element with respect to another, or by judiciously applying Eq. (21) such that a positive nearest-neighbor EPI comes about.

The TB-LMTO approaches successfully describe the variation of the EPI with the e/a ratio. The SK parameters derived from the $B2$ NiAl structure give somewhat less accurate EPI values than those obtained from the pure element TB-LMTO derived SK parameters. The latter give excellent agreement with the KKR-CPA-GPM result. The poorer performance by the $B2$ NiAl derived SK parameters is probably due to the strong ionicity in $B2$ NiAl, which is carried over by the SK parameters into the actually not so ionic disordered bcc structure. We find excellent agreement between the KKR-CPA-GPM results and the corresponding results obtained with the SK parameters of the TB-LMTO method for the whole composition range, and the agreement extends to the angular-momentum-decomposed EPI given by Eq. (20), as is shown in Fig. 5.

The composition dependence of the EPI also is described well by the TB-LMTO as is shown in Fig. 6. Only toward high Ni concentration does a noticeable discrepancy exist, where the results based on the SK parameters obtained with the TB-LMTO method predict an increase in the first-nearest-neighbor EPI with increasing Ni concentration. This is in disagreement with the KKR-CPA-GPM results that indicate an essentially composition-independent first-nearest-neighbor EPI at high Ni content.

IV. CONCLUSIONS

We have shown that the SK parameters obtained from the TB-LMTO formalism have a number of advantages over those obtained from fits to electronic bands. Some of the advantages are: (i) The TB-LMTO potential parameters are structure independent, and hence one LMTO calculation can yield SK parameters for a wide range of crystal structures. (ii) The TB-LMTO SK parameters follow the scaling law, Eq. (1), fairly well. (iii) Unlike the fitted SK parameters, the TB-LMTO SK parameters are defined with reference to the Coulomb potential so that no arbitrary rigid shift of the on-site energies is needed when alloys are considered. (iv) The TB-LMTO SK parameters describe the chemical interactions with remarkable accuracy, unlike the fitted SK parameters.

ACKNOWLEDGMENTS

This work was performed under the auspices of the U.S. Department of Energy by the Lawrence Livermore National Laboratory under Contract No. W-7405-ENG-48.

[1]D. A. Papaconstantopoulos, *Handbook of the Band Structure Elemental Solids* (Plenum, New York, 1986).
[2]O. K. Andersen, O. Jepsen, and D. Glotzel, in *Highlights of Condensed Matter Theory*, Proceedings of the International School of Physics "Enrico Fermi," Course LXXXIX, Varenna, 1983, edited by F. Bassani, F. Fermi, and M. P. Tosi (North-Holland, Amsterdam, 1985), p. 59.
[3]Prabhakar P. Singh, Phys. Rev. B **43**, 3975 (1991).
[4]J. A. Blackman, D. M. Esterling, and N. F. Berk, Phys. Rev. B **4**, 2412 (1971).
[5]A. Gonis and J. W. Garland, Phys. Rev. B **16**, 1495 (1977).
[6]A.-B. Chen, Phys. Rev. B **7**, 2230 (1973).
[7]J. S. Faulkner, in *Progress in Materials Science*, edited by J. W. Christian, P. Haasen, and T. B. Massalski (Pergamon Press, New York, 1982), Vol. 27, p. 1, and references cited therein.
[8]O. K. Andersen, W. Klose, and H. Nohl, Phys. Rev. B **17**, 1209 (1978).
[9]J. D. Shore and D. A. Papaconstantopoulos, Phys. Rev. B **35**, 1122 (1987).
[10]F. Ducastelle, in *Alloy Phase Stability*, Vol. 163 of *NATO Advanced Study Institute Series E: Applied Sciences*, edited by G. M. Stocks and A. Gonis (Kluwer Academic Publishers, Boston, 1989), p. 293, and references cited therein.
[11]M. Sluiter, P. E. A. Turchi, F. J. Pinski, and G. M. Stocks, J. Phase Equilibria **13**, 605 (1992).